Fish and Shellfish Immunology 92 (2019) 889–896

Contents lists available at ScienceDirect

Fish and Shellfish Immunology

journal homepage: www.elsevier.com/locate/fsi

Full length article

Tiger frog virus ORF104R interacts with cellular VDAC2 to inhibit cell apoptosis

Jian He[a,b], Shu Mi[a,b], Xiao-Wei Qin[b,c], Shao-Ping Weng[b,c], Chang-Jun Guo[a,b,c,*], Jian-Guo He[a,b,c]

[a] State Key Laboratory for Biocontrol / Guangdong Provincial Key Laboratory of Marine Resources and Coastal Engineering, School of Marine Sciences, Sun Yat-sen University, No.132 Waihuan Dong Road, Higher Education Mega Center, Guangzhou, Guangdong, 510006, PR China
[b] Southern Laboratory of Ocean Science and Engineering (Guangdong, Zhuhai), Zhuhai, 519000, China
[c] Institute of Aquatic Economic Animals / Guangdong Province Key Laboratory for Aquatic Economic Animals, School of Life Sciences, Sun Yat-sen University, 135 Xingang Road West, Guangzhou, 510275, PR China

ARTICLE INFO

Keywords:
Ranavirus
TFV
Bcl-2
Apoptosis
VDAC2

ABSTRACT

Ranaviruses belong to the family *Iridoviridae*, and have become a serious threat to both farmed and natural populations of fish and amphibians. Previous reports showed that ranaviruses could encode viral Bcl-2 family-like proteins (vBcl-2), which play a critical role in the regulation of cell apoptosis. However, the mechanism of ranaviruses vBcl-2 interactions with host protein in mediating apoptosis remains unknown. Tiger frog virus (TFV) belonging to the genus *Ranavirus* has been isolated from infected tadpoles of *Rana tigrina rugulosa*, and it causes a high mortality rate among tiger frog tadpoles cultured in southern China. This study elucidated the molecular mechanism underlying the interaction of TFV ORF104R with the VDAC2 protein to regulate cell apoptosis. TFV ORF104R is highly similar to other ranaviruses vBcl-2 and host Mcl-1 proteins, indicating that TFV ORF104R is a postulate vBcl-2 protein. Transcription and protein expression levels showed that TFV *orf104r* was a late viral gene. Western blot results suggested that TFV ORF104R was a viral structural protein. Subcellular localization analysis indicated that TFV ORF104R was predominantly colocalized with the mitochondria. Overexpressed TFV ORF104R could suppress the release of cytochrome C and the activities of caspase-9 and caspase-3. These results indicated that TFV ORF104R might play an important role in anti-apoptosis. Furthermore, the interaction between TFV ORF104R and VDAC2 was detected by co-immunoprecipitation *in vitro*. The above observations suggest that the molecular mechanism of TFV-regulated anti-apoptosis is through the interaction of TFV ORF104R with the VDAC2 protein. Our study provided a mechanistic basis for the ranaviruses vBcl-2-mediated inhibition of apoptosis and improved the understanding on how TFV subverts host defense mechanisms *in vivo*.

1. Introduction

Apoptosis is a programmed cell death and an active response controlled by genes. This complex biochemical process results in the death of a cell as a response to environmental changes, physiological pathological stimulation, or chronic injury [1]. Apoptosis can be triggered by extrinsic and intrinsic (or mitochondrial) signaling pathways [2]. The extrinsic pathway is initiated by the ligand-induced oligomerization of specific cell surface receptors, such as Fas/CD95 and the tumor necrosis factor receptor (TNFR). This process induces the intracellular assembly of the death-inducing signaling complex, a molecular platform for activating the caspase cascade from caspase-8 [3]. By contrast, the intrinsic pathway is controlled by the mitochondria, which collect and integrate pro-apoptotic and anti-apoptotic signals coming from other organelles and from the extracellular microenvironment. Progression through the pathway usually leads to the activation of caspase-9, activating the effector caspases and nucleases (e.g., caspase-3 and caspase-activated DNase) [4].

Virus propagation can be resisted effectively by apoptosis. Correspondingly, many viral genes are encoded to inhibit or utilize apoptosis [5]. Many viruses can inhibit apoptosis to escape from elimination by hosts. West Nile virus capsid proteins inhibit apoptosis through the PI3K signaling pathway during virus RNA replication [6]. The Human herpesvirus 6B U20 protein inhibits signal cascade and apoptosis mediated by TNFR [7]. Epstein–Barr virus (EBV) protein EBNA3C can inhibit host cell apoptosis mediated by the E2F1 protein

* Corresponding author. State Key Laboratory for Biocontrol / Guangdong Provincial Key Laboratory of Marine Resources and Coastal Engineering, School of Marine Sciences, Sun Yat-sen University, No.132 Waihuan Dong Road, Higher Education Mega Center, Guangzhou, Guangdong, 510006, PR China.
E-mail address: gchangj@mail.sysu.edu.cn (C.-J. Guo).

https://doi.org/10.1016/j.fsi.2019.07.017
Received 6 November 2018; Received in revised form 6 April 2019; Accepted 8 July 2019
Available online 09 July 2019
1050-4648/

[8]. Fish viruses can also manipulate apoptosis; for instance, the Infection spleen and kidney necrosis virus ORF111L protein interacts with TRADD and induces caspase 8-mediated apoptosis [9], Singapore grouper iridovirus (SGIV) VP51 improves cell viability during SGIV infection by inhibiting virus-induced apoptosis [10], and Grouper iridovirus (GIV) VP27 can inhibit apoptosis through intrinsic and extrinsic pathways [11].

Ranaviruses belong to the family *Iridoviridae*, and have become a serious threat to both farmed and natural populations of fish and amphibians, such as grouper (*Epinephelus coioides*), red-finned perch (*Perca fluviatilis*), mandarin fish (*Siniperca chuatsi*), and tiger frog (*Hoplobatrachus rugulosus*) [12,13]. Tiger frog virus (TFV) belonging to the genus *Ranavirus* has been isolated from infected tadpoles of *Rana tigrina rugulosa*, and it causes a high mortality rate among tiger frog tadpoles cultured in southern China [14]. TFV is the first member of the family *Iridoviridae* to have a complete genome sequence. The genome of this virus comprises double-stranded DNA of 105,057 base pairs in length and is organized by 105 non-overlapping open reading frames (ORFs) [15]. Previous studies showed that ranaviruses could encode Bcl-2 family-like proteins (vBcl-2), such as Frog virus 3 (FV3) ORF97R and GIV ORF066R [16,17]. The function of vBcl-2 in those ranaviruses was also studied. FV3 ORF097R overexpression in baby green monkey kidney cells may induce apoptosis [16,17]. GIV ORF066R can inhibit UV-induced apoptosis in grouper kidney cells at the early stage of GIV infection [16,17]. However, the detailed mechanism by which ranavirus vBcl-2 mediates apoptosis remains unclear.

Thus, this study investigated the mechanism of TFV ORF104R inhibiting cell apoptosis through intrinsic pathways.

2. Materials and methods

2.1. Cells and antibodies

Fathead minnow (FHM) cells (ATCC® CCL-42™) were cultured as a monolayer at 27 °C in M199 medium supplemented with 10% fetal bovine serum. NIH3T3 (ATCC® CRL-1658) and HEK293T (ATCC® CRL-3216) cells were cultured as a monolayer at 37 °C in complete Dulbecco's modified Eagle's medium supplemented with 10% fetal bovine serum. TFV was originally isolated from diseased tadpoles in Naihai, Guangdong, China and maintained in our laboratory. TFV was grown in FHM cells at 27 °C. Mouse polyclonal serum against TFV major capsid protein (MCP) antibody, mouse polyclonal serum against TFV ORF104R protein antibody, and mouse polyclonal serum against TFV ORF020R protein antibody were prepared as previously reported [18,19]. Other antibodies used in this study were as follows: rabbit anti-VDAC1 (Cell Signaling Technology, USA), mouse anti-Myc antibody (Sigma–Aldrich, Germany), rabbit anti-HA antibody (Sigma–Aldrich, Germany), rabbit anti-GAPDH antibody (Sigma–Aldrich, Germany), and anti-β-actin antibody (Sigma–Aldrich, Germany).

2.2. Virus purification and western blot

Confluent monolayers of cells were infected with TFV (MOI = 10) and incubated at 27 °C. At 6 days post-infection (p.i.), the supernatant was harvested before cell detachment, and cell debris was removed by low-speed centrifugation. Virus purification through sedimentation in sucrose density gradients was conducted as previously described [18]. Protein concentrations of the purified virus stocks were determined using the DC protein assay kit (Bio-Rad, USA). Approximately 20 μg of the purified sample was boiled in SDS loading buffer and analyzed by SDS-polyacrylamide gel electrophoresis (PAGE) on a 12% or 15% polyacrylamide gel. Western blot was performed as previously described [20].

2.3. Transcript analysis

To detect the transcription of TFV *orf104r*, we used cycloheximide (CHX, MCE, USA) and cytosine arabinoside (AraC, MCE, USA) to inhibit the de novo protein and DNA syntheses, respectively. In brief, the cells were either pretreated with CHX (200 μg/mL) or AraC (400 μg/mL) for 1 h prior to TFV infection. Mock-treated cells were used as control. Total RNA was extracted and reverse-transcribed to cDNA, followed by PCR. TFV *orf097r*, a previously characterized early (E) gene during TFV infection, and TFV *mcp*, a known late (L) gene, were used as indicative controls [21]. Primers used were as follows: TFV *orf097r*, forward primer: 5′-TGCCACATCCAGACATTC-3′, reverse primer: 5′-CAATCTCT ATCAGCCTCCTT-3′; TFV *mcp* gene, forward primer: 5′-TCGCTGGTGG AGCCCTGGTA-3′, reverse primer: 5′-GGCGTTGGTCAGTCTGCCGTA-3′; TFV *orf104r* forward primer: 5′-ATGGATGTGAGGCAATTTCTGT CAG-3′, reverse primer: 5′-TCAAGAGAACAAGAGAGACAGGATC-3′ and *gapdh* gene forward primer: 5′-ATGGTGAAGGTCGGTGTGAACGG-3′; reverse primer: 5′-TTACTCCTTGGAGGCCATGTAG-3′. The primer sequences of TFV *orf097r* and TFV *mcp* genes were used on the basis of previous studies [22]. The primer sequences of TFV *orf104r* was designed based on the TFV *orf104r* sequence (GenBank accession no. AF389451.1) from the NCBI Nucleotide. The primer sequence of the *gapdh* gene was designed based on the mouse *gapdh* sequence (ENSMUST00000073605.14) from the Ensembl Genomes.

2.4. qRT-PCR

Total RNAs were extracted using the SV Total RNA Isolation System kit (Promega, USA) and treated with RNase-free DNase (Promega, USA) to remove the contaminating DNA. Then, the samples were reverse-transcribed to cDNA using the PrimeScript™ RT reagent kit (TAKARA, Japan). Relative qPCR was performed to determine the relative mRNA level of the TFV *orf104r* gene. The *gapdh* gene was used as an internal control. The transcription levels of TFV *orf104r* were normalized to that of the *gapdh* gene. QRT-PCR was conducted using a LightCycler® 480 instrument (Roche, Germany). The primers were as follows: TFV *orf104r* gene; forward primer: 5′-GCAGGTACATCGTCAGGA-3′; reverse primer: 5′-AGCCTATCTGTCCACTCTC-3′; and *gapdh* gene forward primer: 5′- TGTGGAAGGGCTCATGACCA-3′; reverse primer 5′- CACCA GTGGATGCAGGGATG-3′.

2.5. Co-immunoprecipitation (Co-IP) assay

HEK293T cells were grown in 6 cm^2 dishes and transfected with plasmids. The plasmids were transfected into the HEK293T cells for Co-IP assay with three types of combination (i.e., pCMV-Myc-TFV ORF104R and pCMV-HAa-VDAC2, pCMV-Myc-TFV ORF104R and pCMV-HA, or pCMV-Myc and pCMV-HA-VDAC2). At 24 h post-transfection, the cells were lysed with ice-cold lysis buffer containing 10 mM Tris-HCl pH 7.5, 0.4 M NaCl, 1% NP-40, 0.4% Triton X-100, 0.2% sodium deoxycholate, 1 mM EDTA, and protease inhibitors (Calbiochem, USA) for 30 min. Cellular debris were removed by centrifugation at 12,000 $\times g$ for 15 min at 4 °C. The lysates were immunoprecipitated with corresponding antibodies and subsequently adsorbed onto Pierce™ Protein A/G Magnetic Beads (Rockford, USA). Lysates were then collected by centrifugation and washed extensively with 1 mL of washing buffer (10 mM Tris-HCl, pH 7.5, 0.2 M NaCl, and 1 mM EDTA). Immunoprecipitated proteins were solubilized by boiling in alkaline SDS loading buffer and subjected to SDS-PAGE before analysis by performing immunoblot as described previously.

2.6. TdT-mediated dUTP Nick-end labeling (TUNEL) assay

Apoptosis was detected by TUNEL assay using the One Step TUNEL Apoptosis Assay Kit (Beyotime, China). Less than 2 million cells were accumulated, and samples were washed once by PBS. The mixture was

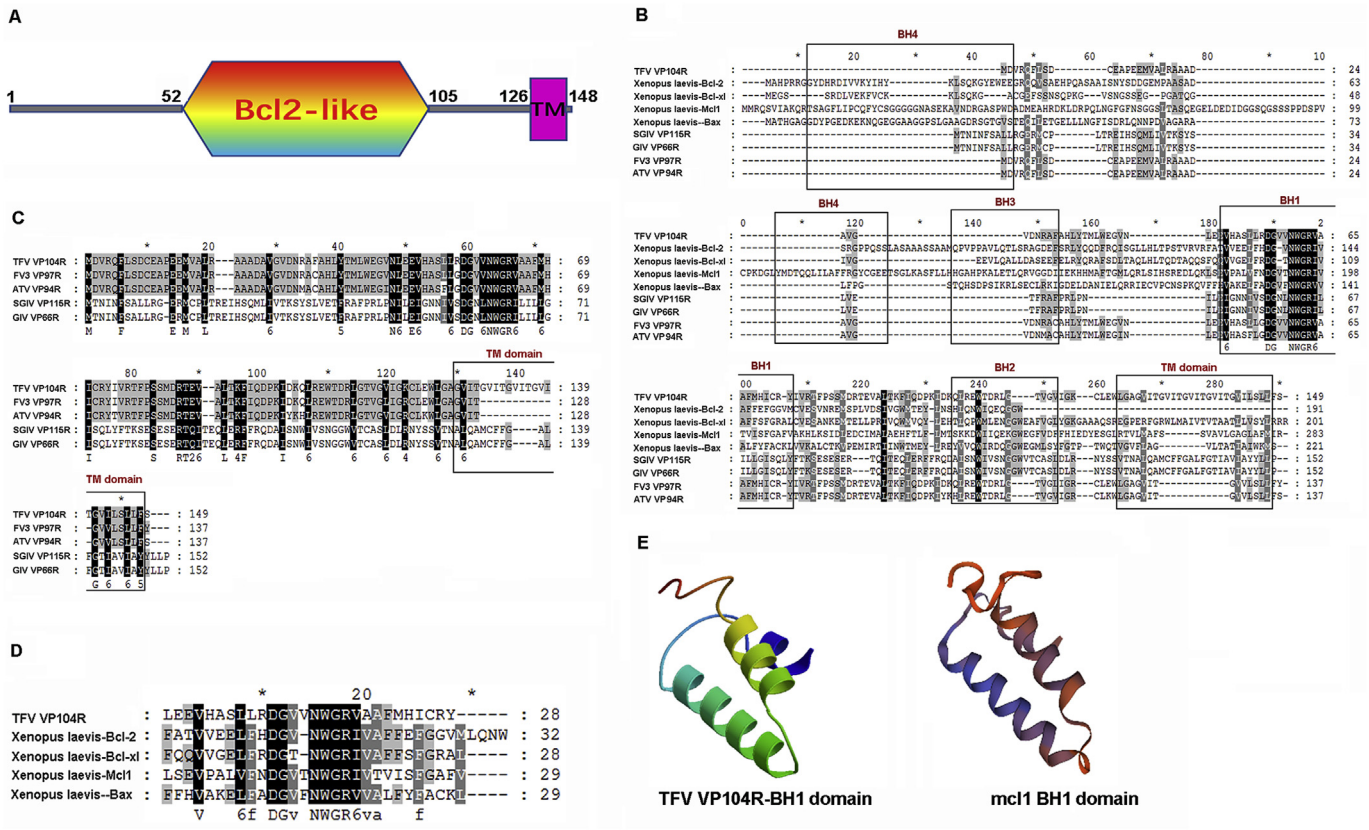

Fig. 1. TFV ORF104R shows high-sequence identity with Bcl-2 family proteins. (A) Analysis of the TFV ORF104R with the NCBI-Blast (https://blast.ncbi.nlm.nih.gov/Blast.) and SMART program (http://smart.embl-heidelberg.de). (B) Multiple-sequence alignment of TFV ORF104R (ABB92349.1) with other iridovirus viral Bcl-2 proteins (YP_164210.1, AAV91093.1, AAT09757.1, YP_003865.1) and four *Xenopus laevis* Bcl-2 family members (XP_002934442, NP_001005428, XP_002935512.1, NP_989185.1) was performed by using the ClustalW program. (C) Multiple-sequence alignment of TFV ORF104R (ABB92349.1) with other iridovirus viral Bcl-2 proteins (YP_164210.1, AAV91093.1, AAT09757.1, YP_003865.1). (D) Multiple-sequence alignment of the BH1 domain of TFV ORF104R (ABB92349.1) with the BH1 domain of four *X. laevis* Bcl-2 family members (XP_002934442, NP_001005428, XP_002935512.1, NP_989185.1). (E) Model structures of the TFV ORF104R BH1 domain (right) and mcl-1 BH1 domain (left) were generated using the SWISS-MODEL Workspace (http://swissmodel.expasy.org/workspace/

added with 4% paraformaldehyde and gradually shaken for 0.5 h to fix the cells, and the samples were washed once with PBS. PBS (containing 0.1% Triton X-100) was added to resuspend the cells, and the mixture was incubated at room temperature for 10 min. The TUNEL detection solution was configured. The TUNEL detection solution (50 μL) for one test was composed of TdT enzyme (5 μL) and fluorescent labeling solution (45 μL). Samples were washed twice with PBS. Then, 50 μL of TUNEL detection solution was added to the samples, and the mixtures were incubated at 37 °C for 1 h. The samples were placed in the dark during incubation. The samples were washed twice with PBS, and then 250–500 μL of PBS or HBSS was added to resuspend the cells. The cells were observed via flow cytometry or fluorescence microscopy. The excitation wavelength of Cy3 was 550 nm, and the emission wavelength was 570 nm (red fluorescence).

2.7. Caspase activity assay

Caspase-3/caspase-9 protease was measured using the Caspase-3/CPP32 Colorimetric Protease Assay (Invitrogen, USA) or Caspase-9/Mch6/Apaf-3 Colorimetric Protease Assay (Invitrogen, USA). Apoptosis was induced in the NIH3T3 cells by treated with CHX (200 μg/mL) for 12 h. A control culture was also incubated but without induction. The cells were counted, and 3–5 × 10^6 cells per sample were formed into pellet. The cells were resuspended in chilled cell lysis buffer and incubated on ice for 10 min. The cells were centrifuged for 1 min in a microcentrifuge (10,000 ×*g*). The supernatant was transferred to a fresh tube and placed on ice. The Quick Start Bradford assay kit (Bio-Rad, USA) was used to determine the protein concentration in a solution. Each supernatant was diluted to a concentration of 50–200 μg protein/50 μL cell lysis buffer (1–4 mg/mL). The number of samples to be measured was determined, and an aliquot sufficient for a 2 × reaction buffer was placed into a tube. DTT was immediately added to the 2 × reaction buffer (10 mM final concentration: 10 μL of 1.0 M DTT stock per 1 mL was added) before use. Then, 50 μL of the 2 × reaction buffer (containing 10 mM DTT) was added to each sample. For the caspase-3 protease assay, 5 μL of the 4 mM DEVD-*p*NA substrate (200 μM final concentration) was added, and the mixture was incubated at 37 °C for 2 h. The samples were stored in the dark during incubation and then read at 405 nm in a microplate reader. For the caspase-9 protease assay, 50 μL of the 2 × reaction buffer (containing 10 mM DTT) was added to each sample. Then, 5 μL of the 4 mM LEHD-*p*NA substrate (200 μM final concentration) was added, and the samples were incubated at 37 °C for 2 h. The samples were stored in the dark during incubation. The samples were read at 405 nm in a microplate reader.

2.8. Mitochondrion extraction and stain

The mitochondrion was extracted using the Cell Mitochondria Isolation Kit (Beyotime, China). MitoTracker Red CMXRos (Invitrogen, USA) was used as follows. NIH3T3 cells were grown in a 24-well plate. When the cells reached the desired confluence, the media were removed from the plate, and pre-warmed (37 °C) staining solution containing MitoTracker probe was added. The samples were incubated for 15–45 min. After staining was completed, the staining solution was replaced with fresh prewarmed media. The cells were observed under a

fluorescence microscope or after staining live cells with a MitoTracker® dye and then fixed and permeabilized for subsequent manipulations.

2.9. Transmission electron microscopy (TEM)

TFV-infected NIH3T3 cells were collected for TEM assays. The cells were first fixed with 2.5% glutaraldehyde in 0.1 M PBS and then in 0.1 M PBS containing 2.0% osmium tetroxide. Ultrathin sections were stained with uranyl acetate-lead citrate and examined on a Philips CM10 electron microscope.

3. Results

3.1. Sequence analysis of TFV ORF104R

The coding region of the TFV *orf104r* gene (GenBank accession no. ABB92349.1) is 450 bp in length (He et al., 2002); the TFV *orf104r* gene was predicted to encode a 149-amino acid peptide (TFV ORF104R). As shown in Fig. 1A, the NCBI-Blast Conserved Domain search and SMART program analysis revealed that TFV ORF104R contains a Bcl-2-like domain (from 52 to 105 aas) and a C-terminal transmembrane domain (from 126 to 148 aas), which is a characteristic of many Bcl-2 family members. However, TFV ORF104R only contains a single BH1 domain (Fig. 1B). The BH1 domain of TFV ORF104R is 48% identical to that of *Xenopus laevis* Bcl-2, 58% to that of *X. laevis* Bcl-xl, 55% to that of *X. laevis* Mcl-1, and 51% to that of *X. laevis* Bax (Fig. 1D). The model structure of the BH1 domain of TFV ORF104R shows high similarity to the human Mcl-1 (Fig. 1E). These observations indicated that the TFV ORF104R may have similar functions to Mcl-1. In addition, TFV ORF104R showed only 35% identity to SGIV ORF115R and 35% to GIV ORF066R (Fig. 1C). By contrast, TFV ORF104R exhibited 89% identity to FV3 ORF097R and 84% to *Ambystoma tigrinum* virus ORF VP94R. Interestingly, TFV ORF104R has a significantly longer TM region than FV3 ORF097R and *A. tigrinum* virus ORF VP94R (Fig. 1C). These results indicate that TFV ORF104R is a postulate vBcl-2 protein (TFV vBcl-2).

3.2. Transcriptional level analysis of the TFV orf104r gene

We performed qRT-PCR using TFV-infected cells at different infection stages to detect the transcription of TFV *orf104r*. As shown in Fig. 2A, the mRNA levels of TFV *orf104r* increased at 6 h post-infection (p.i.). With prolonged time and increasing infection, the change in level became 24 times at 8 h and 224 times at 12 h. Western blot analysis was performed to detect the levels of the TFV ORF104R protein at different time points after infection with TFV (Fig. 2B). TFV ORF104R was initially detected at 6 h p. i., and the intensity of the bands increased at 96 h p.i. Furthermore, to determine whether TFV *orf104r* is an immediate-early, delay-early, or late (IE, DE, or L) gene, we used cyclohexane (CHX) and cytarabine (AraC) in drug inhibition assays. CHX and AraC can inhibit protein or DNA synthesis, respectively. These molecules were used to classify the transcripts of iridovirus genes as IE, DE, or L genes. As shown in Fig. 2C, the transcription of TFV *orf097r* (an IE gene) was not affected by CHX or AraC, whereas that of TFV *mcp* (an L gene) was inhibited significantly in the presence both drugs. The transcription pattern of TFV *orf104r* was similar to that of TFV *mcp* (Fig. 2C). Both drug treatments affected its transcription, indicating that TFV *orf104r* is a viral L gene. These results suggest that TFV ORF104R is a late viral protein.

3.3. TFV ORF104R is a structural protein of virion particles

Virus structural proteins, as the component of mature virion particles, are of high interest in functional investigations of viruses because they play a crucial role in viral infections. Mature virions could be purified from infected cells by sucrose density gradients (Fig. 3A). TFV ORF104R was detected in the purified TFV virions by Western blot to identify whether TFV ORF104R is a virus structural protein. The results showed that TFV ORF104R was detected in the purified TFV virions (Fig. 3B, lane 1, up plate), suggesting that TFV ORF104R is a viral structural protein. Ranavirus particles consist of a naked virion and an outer viral envelope. We prepared supernatant and pellet fractions of viral proteins with 0.5% Triton X-100 to investigate the localization of TFV ORF104R in the virions. The viral structural proteins were in the pellet, and envelope proteins were in the supernatant fractions. Structural protein MCP and envelope protein VP020R were used as controls [18]. The prepared samples were analyzed by Western blot. TFV ORF104R, MCP, and VP020R were detected in the purified virions (Fig. 3B, lane 1). TFV ORF104R and MCP were mostly present in the pellet fraction (Fig. 3B, lane 2), whereas VP020R was predominantly detected in the supernatant fraction (Fig. 3B, lane 3, envelope protein). These results suggest that TFV ORF104R is a viral structural protein but not a viral envelope protein. Thus, TFV ORF104R was located in the TFV naked-virion rather than in the viral envelope.

3.4. Subcellular localization of TFV ORF104R

TFV ORF104R contains a Bcl-2 family-like domain structure. Thus, we speculated that the protein may be located in the mitochondria. We transfected the pCMV-Myc-TFV104R recombinant plasmid into the NIH3T3 cells to observe the cellular localization of TFV ORF104R. MitoTracker Red CMXRos was used to stain the mitochondria at 24 h post-transfection (p.t.). The subcellular localization of TFV ORF104R was observed using a confocal microscope. The green fluorescence represents Myc-TFV ORF104R, whereas the red fluorescence represents the mitochondria (Fig. 4B). In the cytoplasm, high orange fluorescence suggests that myc-TFV ORF104R was colocalized with the mitochondria. Moreover, cells were transfected with the myc-TFV ORF104R recombinant plasmids and then collected to extract the mitochondria after 24 h p.t.. The voltage-dependent anion channel 1 (VDAC1) protein was used as a mitochondrial marker protein, and β-actin was used as a cytoplasmic marker. As shown in Fig. 4B, VDAC1 was abundant in the mitochondrial component but very weak in the cytoplasmic component; β-actin was abundant in the cytoplasmic component but very weak in the mitochondrial component. Those results indicated that the extracted mitochondria were relatively pure. Myc-TFV ORF104R recombinant proteins were detected in the mitochondria by Western blot. Most Myc-TFV ORF104R recombinant proteins were detected in the mitochondria fraction, and a few Myc-TFV ORF104R recombinant proteins were detected in the cytoplasmic fraction (Fig. 4A). These results indicate that TFV ORF104R is mainly overexpressed the cellular mitochondria.

3.5. Intrinsic apoptosis inhibition by TFV ORF104R

TFV ORF104R is a vBcl-2 protein located in the cellular mitochondria, suggesting that this protein participates in the intrinsic pathway of apoptosis. The TFV ORF104R-EGFP recombinant plasmid was transfected into NIH3T3 cells to observe the direct influence of TFV ORF104R on apoptosis, and the pEGFP-N3 plasmid was used as a control. After 24 h p.t., all green-fluorescent-positive cells were filtered through the separation flow cytometry instrument. After flow cytometry, CHX (200 μg/mL) was added to induce cell apoptosis. After 12 h of induction, the apoptosis index was detected. TUNEL detection results showed that the apoptosis rate was 0.8% in the NIH3T3 cells expressing the TFV ORF104R-EGFP recombinant protein after induction, whereas the apoptosis rate was as high as 3.6% in the cells expressing the EGFP protein (Fig. 5A). Release of cytochrome C from the mitochondria is an important characteristic of apoptosis. The cells expressing the TFV ORF104R-EGFP recombinant or EGFP protein were collected to extract the mitochondria. The amount of cytochrome C was detected in the mitochondria by Western blot. The amount of cytochrome C released from the mitochondria to the cytoplasm in the cells expressing the TFV

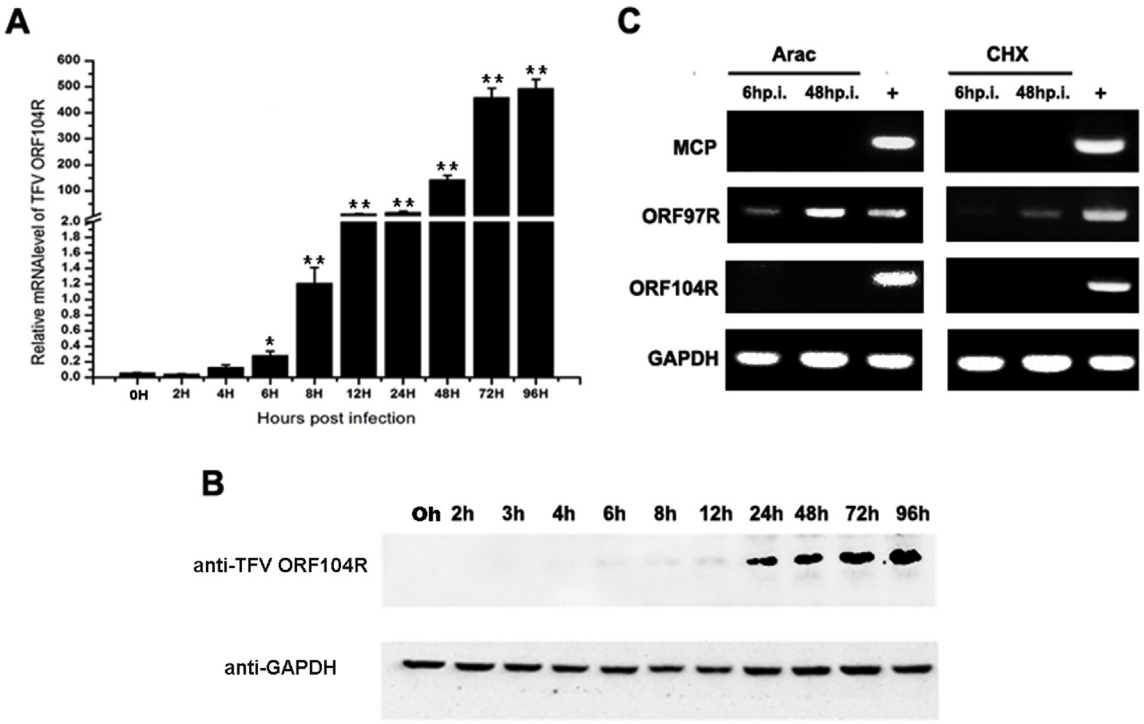

Fig. 2. Relative qRT-PCR and Western blot analyses of the expression of ORF104R. (A) Expression of TFV ORF104R in TFV-infected cells at different time points was determined by relative qRT-PCR and quantified relative to *gapdh* amplified from the same RNA sample as a control. The abscissa indicates the different times (hours p.i.), whereas the ordinate indicates the change in transcription level in TFV *orf104r*. All data were analyzed by unpaired sample *t*-test. Error bars represent the mean ± S.D. (n = 3). $^{**}p < 0.01$, $^{*}p < 0.05$. (B) Cells were infected with TFV in the presence of CHX or AraC, and the transcripts were assayed by qRT-PCR at 6 and 48 h p.i. (C) Temporal expression pattern of the TFV ORF104R protein in TFV-infected cells by Western blot analysis using mouse anti-TFV ORF104R. GAPDH were used as internal controls.

ORF104R-EGFP recombinant was less than those of the cells expressing the EGFP protein (Fig. 5D). Furthermore, the activities of caspase-9 and caspase-3 were investigated. Cells expressing the EGFP protein or the TFV ORF104R-EGFP-recombinant protein were induced by CHX. Then, the activities of caspase-9 (Fig. 5C) and caspase-3 (Fig. 5B) were detected. The corresponding activities were significantly ($p < 0.05$) inhibited by 57.2% and 40.3% in the cells expressing the TFV ORF 104R-EGFP-recombinant protein than in the cells expressing EGFP protein. These results indicate that TFV ORF104R can inhibit apoptosis in NIH3T3 cells.

3.6. Interaction of TFV ORF104R with the VDAC2 protein

To investigate the molecular mechanism by which TFV ORF104R inhibits cell apoptosis, we identified the cellular protein that interacts with TFV ORF104R by protein–protein interaction assay. After a preliminary screening, we used pull-down experiment (data not shown) and found that TFV ORF104R might interact with the cellular VDAC2 protein. The interaction between VDAC2 and TFV ORF104R was identified using Co-IP experiments. HEK293 cells were transiently transfected to produce HA-tagged VDAC2 protein and Myc-tagged TFV ORF104R. The recombinant proteins (HA-tagged VDAC2 protein and Myc-tagged TFV ORF104R) were overexpressed in the cells, as shown in the input lanes (Fig. 6, lanes 2, 4, and 6, respectively). Immunoprecipitation of Myc-tagged ORF104R was detected using Myc tag-specific monoclonal antibody, which led to the coprecipitation of HA-tagged VDAC2 protein (Fig. 6, lane 3). In the converse experiment, immunoprecipitation of the HA-tagged VDAC2 protein was detected using HA-tag specific monoclonal, which resulted in the coprecipitation of Myc-tagged TFV ORF104R (Fig. 6, lane 3). These results suggest that TFV ORF104R interacts with VDAC2.

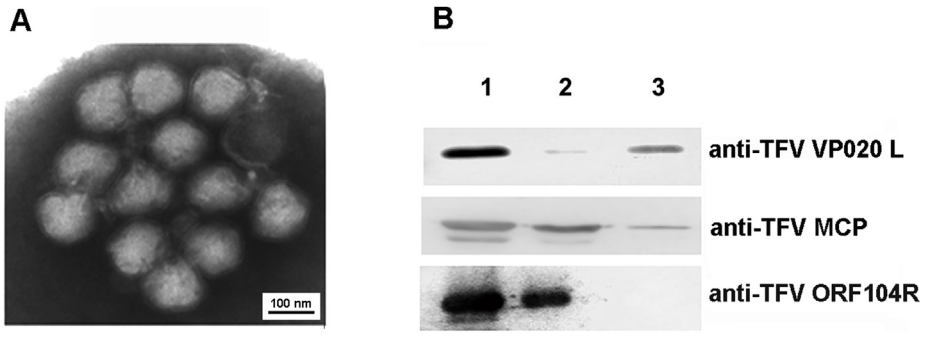

Fig. 3. Localization of TFV ORF104R on TFV virion. (A) Purified TFV virion observed by transmission electron microscopy. (B) Detection of TFV ORF104R on TFV virion by Western blot. Untreated purified virions as positive control (lane 1), Purified virions were subjected to 0.5% Triton X-100 as detergent treatments, followed by centrifugation, thereby resulting in separated pellet, supernatant–viral structural protein (lane 3), and envelope protein (lane 2). The viral structural protein MCP and envelope protein VP020R were used as positive controls to indicate the complete separation of the two types of proteins. The two fractions and whole purified TFV virions were subjected to Western blot using anti-TFV ORF104R, anti-MCP, and anti-VP020R antibodies.

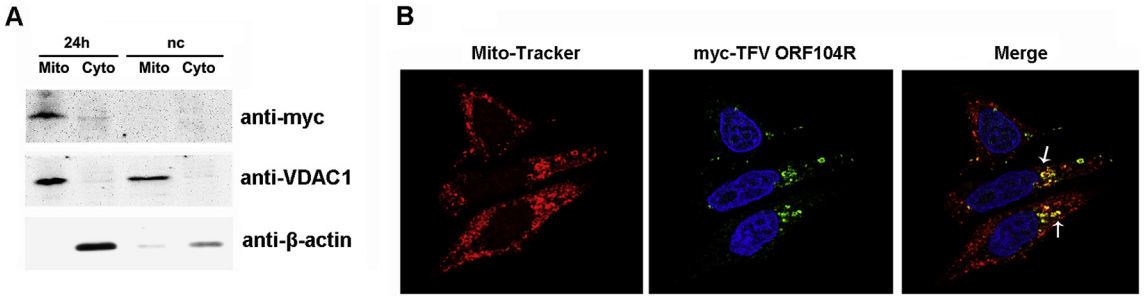

Fig. 4. Subcellular localization of TFV ORF104R in NIH3T3 cells. (A) Transfected pCMV-Myc-TFV104R recombinant plasmid into NIH3T3 cells. At 24 h post-transfection, NIH3T3 cells were collected to extract the mitochondria. Western blot detected Myc-ORF104R in the mitochondria (Mito) and cytoplasm (Cyto), VDAC1 was used as a mitochondrial marker, and β-actin was used as a cytoplasmic marker. (B) Transfected pCMV-Myc-TFV104R recombinant plasmid into NIH3T3 cells. At 24 h post-transfection, MitoTracker Red CMXRos was used to stain the mitochondria, and red represents the mitochondria; immunofluorescence assay was employed to detect Myc-TFV ORF104R in the stained cells, and green represents Myc-TFV ORF104R; the yellow overlay represents the colocalization of Myc-TFV ORF104R and mitochondria (white arrows).

4. Discussion

Apoptosis is a potent defense mechanism deployed by higher organisms against viruses. In turn, viruses have evolved an astonishing array of strategies to ensure their successful proliferation, propagation, and survival. Bcl-2 family members play a critical role in the regulation of cell apoptosis. Bcl-2 family proteins are mainly divided into two categories, namely, anti-apoptotic proteins (e.g., Bcl-2, Bcl-xl, and Mcl-1) and pro-apoptotic proteins (e.g., BAX and BAK) [23]. Viruses could encode the viral Bcl-2 protein to mediate host apoptosis. Vaccinia virus encodes a family of Bcl-2, such as protein F1L, which can interact with pro-apoptotic protein to inhibit apoptosis [24]. BALF1 and BHRF1 encoded by EBV belong to the Bcl-2-like family and can inhibit apoptosis [25,26].

Ranaviruses also encode vBcl-2-like proteins, such as FV3 ORF97R and GIV ORF066R [16,17]. The sequenced analysis showed that TFV ORF104R was a vBcl-2 protein (Fig. 1A). Bcl-2-related proteins share homology in one to four regions designated the Bcl-2 homology (BH) domains BH1, BH2, BH3 and BH4 [27]. Through the multiple sequence alignment with TFV ORF104R, other ranaviruses vBcl-2 proteins, and *X. laevis* Bcl-2 family proteins, we found that the TFV ORF104R protein only contains one BH1 domain and one transmembrane domain in the protein (Fig. 1B). In defining and classifying members of this superfamily on the basis of function and domain structure, two facts emerge. First, proteins that inhibit apoptosis harbor at least three BH domains (BH1, BH2, and BH3) as well as a transmembrane domain; second, the minimum requirement for a death-promoting protein is a BH3 domain [28]. Furthermore, the model structure of the BH1 domain of TFV ORF104R (Fig. 1E) shows high similarity to the human Mcl-1 (an anti-apoptosis protein). Thus, all the sequence information indicated that TFV ORF104R is another ranavirus vBcl-2 protein with similarity to the myeloid cell leukemia-1 (Mcl-1) protein and that the function of TFV ORF104R is anti-apoptosis.

In the present study, the characteristics of TFV ORF104R were investigated. We confirmed that TFV *orf104r* is a viral L gene in the presence of CHX (an inhibitor de novo of protein synthesis) or AraC (an inhibitor of viral DNA synthesis) (Fig. 2). Previous studies showed that ranavirus vBcl-2 proteins have different expression patterns. GIV vBcl-2 is an IE gene, whereas FV3 ORF097R is an IE-S gene [16,17]. The expression profile of TFV *orf104r* is different from those of other known ranavirus *vBcl-2* genes. As previously described, the GIV vBcl-2 protein is a structural protein of GIV [16,17]. However, no evidence has been found to define FV3 ORF097R. Moreover, we identified that TFV ORF104R is a viral structural protein and further found that TFV ORF104R is not a viral envelope protein (Fig. 3). We analyzed the TFV ORF104R subcellular location in the infected cells and revealed that TFV ORF104R was predominantly colocalized with the mitochondria at 24 h post-transfection (Fig. 4). TFV ORF104R exhibited 93% identity to

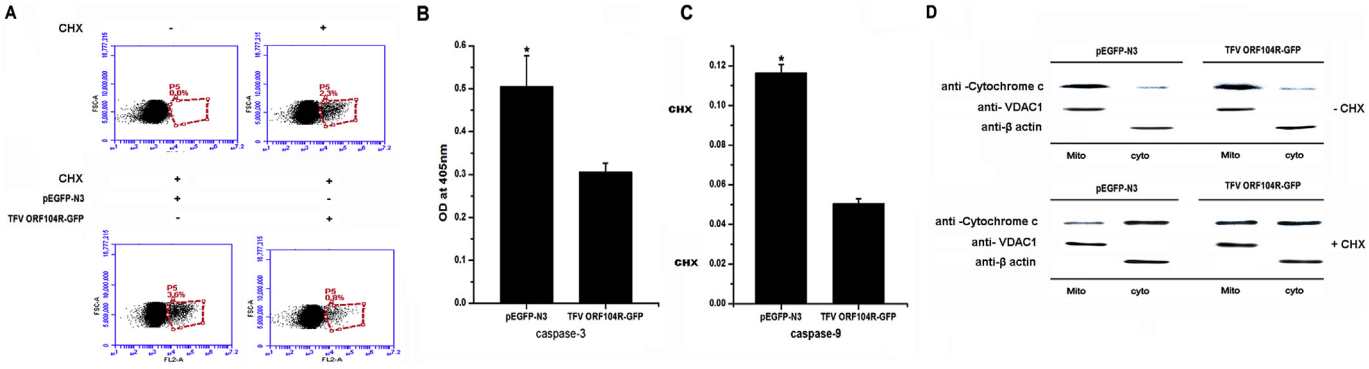

Fig. 5. TFV ORF104R protein protects NIH3T3 cells from CHX-induced apoptosis. The ORF104R-EGFP recombinant plasmids were transfected into NIH3T3 cells, and the pEGFP-N3 plasmid was used as a control. After 24 h transfection, all green fluorescence positive cells were filtered through the separation flow cytometry instrument and cultured 12 h after separation. (A) NIH3T3 cells expressing ORF104R-EGFP and EGFP were treated with CHX (200 μg/mL) for 12 h to induce apoptosis, and then TUNEL assay was used to detect apoptotic cells, followed by flow cytometry analysis. (B) NIH3T3 cells expressing ORF104R-EGFP and EGFP were treated with CHX (200 μg/mL) for 12 h to induce apoptosis. Then, the activity of caspase-9 was detected. $^*p < 0.05$ as compared with the control group. (C) NIH3T3 cells expressing ORF104R-EGFP and EGFP were treated with CHX (200 μg/mL) for 12 h to induce apoptosis. Then, the activity of caspase-3 was detected. $^*p < 0.05$ as compared with the control group. (D) NIH3T3 cells expressing ORF104R-EGFP and EGFP were treated with CHX (200 μg/mL) for 12 h; the mitochondria were isolated from each group of cells; Western blot detected the cytochrome C in the mitochondria or cytoplasm, VDAC1 was used as a mitochondrial marker, and β-actin was used as a cytoplasmic marker.

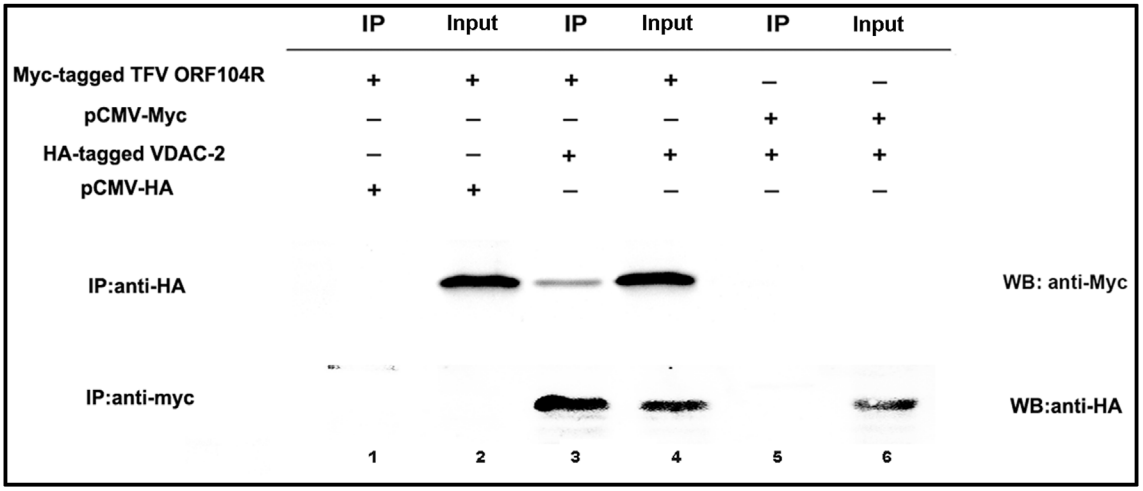

Fig. 6. VDAC2 interacts with TFV ORF104R. HEK293T cells were transiently transfected with Myc-tagged TFV ORF104R and pCMV-HA empty vector (lanes 1 and 2), HA-tagged VDAC2 protein and Myc-tagged TFV ORF104R (lanes 3 and 4), and pCMV-Myc empty vector and HA-tagged VDAC2 protein (lanes 5 and 6), respectively, as indicated (lane 3). Immunoprecipitation (IP) of Myc-tagged TFV ORF104R with Myc tag-specific monoclonal antibody led to the co-IP of the HA-tagged VDAC2 protein. IP of VDAC2 protein HA-tagged using HA-tag-specific monoclonal resulted in the co-IP of Myc-tagged TFV ORF104R.

FV3 ORF097R, but they have different subcellular locations. FV3 ORF097R localized to the endoplasmic reticulum (ER) at 24 h post-transfection. However, at 35 h post-transfection, ORF097R localized to the ER but also began to form concentrated pockets continuous with the nuclear membrane [16,17]. The transmembrane domain of FV3 ORF097R is the reason for the localization of ORF097R to the ER [16,17]. TFV ORF104R and FV3 ORF097R have very high homologies, but they remarkably differ in the C section of the TM domain (Fig. 2B). Those characteristics might cause the distinct subcellular locations of TFV ORF104R and FV3 ORF097R.

Ranavirus vBcl-2 proteins could regulate apoptosis, but the underlying mechanism remains unknown. GIV vBcl-2 could inhibit cell apoptosis during the early stage of GIV infection [16,17]. Over-expressed FV3 ORF097R invaginates the ER and the outer nuclear membrane into the nucleoplasm. These phenomena may be associated with FV3-induced apoptosis [16,17]. As well known, ranaviruses infect a wide range of cell lines, not only including fish cell lines such as FHM cells and zebrafish embryonic fibroblast (ZF4) cells [19], but also mammalian cell lines, such as HepG2, BHK-21 [29], and NIH3T3 (Fig. S1). Considering the efficiency of cell transfection and the use of commercialized antibodies, we investigated the detailed mechanism by which TFV ORF104R mediates apoptosis in NIH3T3 cells. Results showed that TFV ORF104R inhibited apoptosis (Fig. 5A). Analysis of the caspase activities showed that TFV ORF104R could inhibit the activities of caspase-9 and caspase-3 after the cells were induced by CHX (Fig. 5B). These results indicate that TFV ORF104R can inhibit apoptosis by the intrinsic pathway. Furthermore, the molecular mechanism by which TFV ORF104R inhibits cell apoptosis was investigated by protein–protein interaction assay. Results showed that TFV ORF104R interacted with VDAC2 (Fig. 6). Accumulating evidence indicated that the VDAC family of proteins is involved in the release of apoptotic proteins via the OMM [30]. The VDAC family of proteins includes three isoforms, namely, VDAC1, VDAC2, and VDAC3, all of which are located on the OMM [31]. VDAC proteins are important in mitochondrion-mediated apoptosis by participating in the release of apoptotic proteins in the intermembrane space and as the proposed targets of pro-apoptotic and anti-apoptotic members of the Bcl-2 family [32]. In the present study, cells expressing the TFV ORF104R-EGFP recombinant protein effectively suppressed the release of cytochrome C from the mitochondria after CHX-induced apoptosis (Fig. 5D). Hence, we speculated that TFV ORF104R inhibits the intrinsic apoptosis by interacting with VDAC2.

In summary, TFV ORF104R encodes a 149-amino acid protein that is associated with the Bcl-like homolog. TFV ORF104R is an L gene that encodes viral structural protein. TFV ORF104R interacts with cellular VDAC2 protein, which is localized to the cellular mitochondria, and inhibits apoptosis in NIH3T3 cells. These results suggest that TFV ORF104R interacts with the cellular VDAC2 protein and inhibits cell apoptosis *in vitro*. Our findings provide a mechanistic basis for the ranavirus vBcl-2-mediated inhibition of apoptosis and improve the understanding on how TFV subverts host defense mechanisms *in vivo*. Considering the lack of suitable experimental animal (*African xenopus*) and frog cell lines, we will study how TFV subverts host defense mechanisms *in vivo* in further studies.

Acknowledgement

This work was supported by the National Key Research and Development Program of China (Nos. 2018YFD0900504 and 2018YFD0900501), the National Natural Science Foundation of China (No. 31702381), the Guangdong Natural Science Foundation (No. 2014TQ01N303), the Science and Technology Planning Project of Guangzhou (Nos. 201607020014 and 201904020043), the China Agricultural Research System (No. CARS-46), the Guangdong Key Research and Development Program (No.2019B020217001), the Guangdong Natural Science Foundation (No. 2016B020202001), the Guangdong Provincial Special Fund for Modern Agriculture Industry Technology Innovation Teams, and the FoShan Natural Science Foundation (No. 20141141020008).

Appendix A. Supplementary data

Supplementary data to this article can be found online at https://doi.org/10.1016/j.fsi.2019.07.017.

References

[1] N.N. Danial, S.J. Korsmeyer, Cell death: critical control points, Cell 116 (2004) 205–219.
[2] J.E. Kokoszka, K.G. Waymire, S.E. Levy, J.E. Sligh, J. Cai, D.P. Jones, et al., The ADP/ATP translocator is not essential for the mitochondrial permeability transition pore, Nature 427 (2004) 461–465.
[3] D. Wallach, T.B. Kang, A. Kovalenko, The extrinsic cell death pathway and the elan mortel, Cell Death Differ. 15 (2008) 1533–1541.
[4] N. Zamzami, G. Kroemer, The mitochondrion in apoptosis: how Pandora's box opens, Nat. Rev. Mol. Cell Biol. 2 (2001) 67–71.
[5] L. Galluzzi, C. Brenner, E. Morselli, Z. Touat, G. Kroemer, Viral control of mitochondrial apoptosis, PLoS Pathog. 4 (2008) e1000018.

[6] M.D. Urbanowski, T.C. Hobman, The West Nile virus capsid protein blocks apoptosis through a phosphatidylinositol 3-kinase-dependent mechanism, J. Virol. 87 (2013) 872–881.
[7] E. Kofod-Olsen, K. Ross-Hansen, M.H. Schleimann, D.K. Jensen, J.M. Moller, B. Bundgaard, et al., U20 is responsible for human herpesvirus 6B inhibition of tumor necrosis factor receptor-dependent signaling and apoptosis, J. Virol. 86 (2012) 11483–11492.
[8] A. Saha, J. Lu, L. Morizur, S.K. Upadhyay, MP. Aj, E.S. Robertson, E2F1 mediated apoptosis induced by the DNA damage response is blocked by EBV nuclear antigen 3C in lymphoblastoid cells, PLoS Pathog. 8 (2012) e1002573.
[9] B.L. He, J.M. Yuan, L.Y. Yang, J.F. Xie, S.P. Weng, X.Q. Yu, et al., The viral TRAF protein (ORF111L) from infectious spleen and kidney necrosis virus interacts with TRADD and induces caspase 8-mediated apoptosis, PLoS One 7 (2012) e37001.
[10] Y. Yu, Y. Huang, S. Wei, P. Li, L. Zhou, S. Ni, et al., A tumour necrosis factor receptor-like protein encoded by Singapore grouper iridovirus modulates cell proliferation, apoptosis and viral replication, J. Gen. Virol. 97 (2016) 756–766.
[11] C.W. Chen, M.S. Wu, Y.J. Huang, P.W. Lin, C.J. Shih, F.P. Lin, et al., Iridovirus CARD protein inhibits apoptosis through intrinsic and extrinsic pathways, PLoS One 10 (2015) e129071.
[12] S.J. Price, E. Ariel, A. Maclaine, G.M. Rosa, M.J. Gray, J.L. Brunner, et al., From fish to frogs and beyond: impact and host range of emergent ranaviruses, Virology 511 (2017) 272–279.
[13] I. Bandin, C.P. Dopazo, Host range, host specificity and hypothesized host shift events among viruses of lower vertebrates, Vet. Res. 42 (2011) 67.
[14] S.P. Weng, J.G. He, X.H. Wang, L. Lü, M. Deng, S.M. Chan, Outbreaks of an iridovirus disease in cultured tiger frog, Rana tigrina rugulosa in Southern China, J. Fish Dis. vol. 25, (2002) 423–427.
[15] J.G. He, L. Lu, M. Deng, H.H. He, S.P. Weng, X.H. Wang, et al., Sequence analysis of the complete genome of an iridovirus isolated from the tiger frog, Virology 292 (2002) 185–197.
[16] B.A. Ring, L.A. Ferreira, D.J. Drummond, C. Wangen, H.E. Eaton, C.R. Brunetti, Frog virus 3 open reading frame 97R localizes to the endoplasmic reticulum and induces nuclear invaginations, J. Virol. 87 (2013) 9199–9207.
[17] P.W. Lin, Y.J. Huang, J.A. John, Y.N. Chang, C.H. Yuan, W.Y. Chen, et al., Iridovirus Bcl-2 protein inhibits apoptosis in the early stage of viral infection, Apoptosis 13 (2008) 165–176.
[18] Q. Wang, Y. Luo, J. Xie, C. Dong, S. Weng, H. Ai, et al., Identification of two novel membrane proteins from the Tiger frog virus (TFV), Virus Res. 136 (2008) 35–42.
[19] Y. Luo, S. Weng, Q. Wang, X. Shi, C. Dong, Q. Lu, et al., Tiger frog virus can infect zebrafish cells for studying up- or down-regulated genes by proteomics approach, Virus Res. 144 (2009) 171–179.
[20] M.M. Hill, M. Bastiani, R. Luetterforst, M. Kirkham, A. Kirkham, S.J. Nixon, et al., PTRF-Cavin, a conserved cytoplasmic protein required for caveola formation and function, Cell 132 (2008) 113–124.
[21] J.F. Xie, Y.X. Lai, L.J. Huang, R.Q. Huang, S.W. Yang, Y. Shi, et al., Genome-wide analyses of proliferation-important genes of Iridovirus-tiger frog virus by RNAi, Virus Res. 189 (2014) 214–225.
[22] Y.S. Chen, N.N. Chen, X.W. Qin, S. Mi, J. He, Y.F. Lin, et al., Tiger frog virus ORF080L protein interacts with LITAF and impairs EGF-induced EGFR degradation, Virus Res. 217 (2016) 133–142.
[23] D.T. Chao, S.J. Korsmeyer, BCL-2 family: regulators of cell death, Annu. Rev. Immunol. 16 (1998) 395–419.
[24] C.A. Ray, R.A. Black, S.R. Kronheim, T.A. Greenstreet, P.R. Sleath, G.S. Salvesen, et al., Viral inhibition of inflammation: cowpox virus encodes an inhibitor of the interleukin-1 beta converting enzyme, Cell 69 (1992) 597–604.
[25] D.S. Bellows, M. Howell, C. Pearson, S.A. Hazlewood, J.M. Hardwick, Epstein-Barr virus BALF1 is a BCL-2-like antagonist of the herpesvirus antiapoptotic BCL-2 proteins, J. Virol. 76 (2002) 2469–2479.
[26] S. Henderson, D. Huen, M. Rowe, C. Dawson, G. Johnson, A. Rickinson, Epstein-Barr virus-coded BHRF1 protein, a viral homologue of Bcl-2, protects human B cells from programmed cell death, Proc. Natl. Acad. Sci. U. S. A. 90 (1993) 8479–8483.
[27] J.K. Brunelle, A. Letai, Control of mitochondrial apoptosis by the Bcl-2 family, J. Cell Sci. 122 (2009) 437–441.
[28] A. Kelekar, C.B. Thompson, Bcl-2-family proteins: the role of the BH3 domain in apoptosis, Trends Cell Biol. 8 (1998) 324–330.
[29] C.J. Guo, D. Liu, Y.Y. Wu, X.B. Yang, L.S. Yang, S. Mi, et al., Entry of tiger frog virus (an Iridovirus) into HepG2 cells via a pH-dependent, atypical, caveola-mediated endocytosis pathway, J. Virol. 85 (2011) 6416–6426.
[30] C.A. Mannella, Minireview: on the structure and gating mechanism of the mitochondrial channel, Vdac, J. Bioenerg. Biomembr. 29 (1997) 525–531.
[31] C.A. Mannella, Conformational changes in the mitochondrial channel protein, VDAC, and their functional implications, J. Struct. Biol. 121 (1998) 207–218.
[32] S. Shimizu, M. Narita, Y. Tsujimoto, Bcl-2 family proteins regulate the release of apoptogenic cytochrome c by the mitochondrial channel VDAC, Nature 399 (1999) 483–487.